Journal of Applied Polymer Science

Preparation of dual-layer acetylated methyl cellulose hollow fiber membranes via co-extrusion using thermally induced phase separation and non-solvent induced phase separation methods

Hanna Jang,[1] Du-Hyun Song,[1] Hye-Jin Lee,[1] Seong-Han Lim,[2] In-Chul Kim,[1] Young-Nam Kwon[3]

[1]Research Center for Biobased Chemistry, Korea Research Institute of Chemical Technology, P.O. Box 107, Sinseongno 19, Yuseong, Daejeon 305-600, Republic of Korea

[2]Manufacturing R&D Center, Hyosung, Anyang 431-080, Republic of Korea

[3]School of Urban & Environmental Engineering, Ulsan National Institute of Science and Technology (UNIST), Ulsan 689-798, Republic of Korea

Correspondence to: I.-C. Kim (E-mail: ickim@krict.re.kr) and Y.-N. Kwon (E-mail: kwonyn@unist.ac.kr)

ABSTRACT: Dual-layer acetylated methyl cellulose (AMC) hollow fiber membranes were prepared by coupling the thermally induced phase separation (TIPS) and non-solvent induced phase separation (NIPS) methods through a co-extrusion process. The TIPS layer was optimized by investigating the effects of coagulant composition on morphology and tensile strength. The solvent in the aqueous coagulation bath caused both delayed liquid–liquid demixing and decreased polymer concentration at the membrane surface, leading to porous structure. The addition of an additive (triethylene glycol, (TEG)) to the NIPS solution resolved the adhesion instability problem of the TIPS and NIPS layers, which occurred due to the different phase separation rates. The dual-layer AMC membrane showed good mechanical strength and performance. Comparison of the fouling resistance of the AMC membranes with dual-layer polyvinylidene fluoride (PVDF) hollow fiber membranes fabricated with the same method revealed less fouling of the AMC than the PVDF hollow fiber membrane. This study demonstrated that a dual-layer AMC membrane with good mechanical strength, performance, and fouling resistance can be successfully fabricated by a one-step process of TIPS and NIPS. © 2015 Wiley Periodicals, Inc. J. Appl. Polym. Sci. **2015**, *132*, 42715.

KEYWORDS: applications; membranes; synthesis and processing

Received 17 March 2015; accepted 7 July 2015

DOI: 10.1002/app.42715

INTRODUCTION

Cellulose is an outstanding membrane material due to its low cost, as well as natural hydrophilic and good mechanical properties.[1] In particular, membranes made of cellulose esters[2–5] have gained wide use owing to their superior resistance to membrane fouling and chlorine degradation compared with other membranes made of polysulfone (PSf), polyvinylidene fluoride (PVDF), and so on.[6–9] However, the cellulose esters have lower mechanical properties due to their lower molecular weight.[5] Therefore, there has been a strong demand for the development of new cellulosic membrane materials with excellent mechanical strength. Most cellulose ester membranes have been fabricated using this non-solvent induced phase separation (NIPS) process. The NIPS process uses the separation of a homogeneous solution into two phases through the exchange of solvent and non-solvent during precipitation,[10] thus allowing the process to be applied to various polymers which are miscible with a solvent.[11] The membrane structure and performance are usually determined by the exchange rate.[12] The NIPS process is a simple and convenient method for the fabrication of membranes, but the membranes so prepared have intrinsically weak mechanical strength.

However, membranes prepared by the thermally induced phase separation (TIPS) process displayed good mechanical strength.[13,14] In the TIPS process, a homogeneous solution separates into two phases when the elevated temperature of the solution decreases, until binodal is reached.[12] Thus, the process has been applied to several semi-crystalline polymers, including polypropylene (PP),[15,16] Poly(ethylene chlorotrifluoroethylene) (ECTFE),[17,18] and poly(vinylidene fluoride) (PVDF).[19,20] Recently, hydrophilic materials of cellulose acetate (CA),[21] cellulose acetate butyrate (CAB),[22,23] poly(methyl methacrylate) (PMMA),[24] and polyacrylonitrile (PAN)[25] were used for the fabrication of porous membranes by the TIPS process.

Table I. Spinning Conditions of AMC Hollow Fibers

	TIPS	TIPS/NIPS	
Dope solution of TIPS (wt %)	AMC/TEG (25 : 75)	AMC/TEG (25 : 75)	PVDF/GBL (40/60)
Dope solution of NIPS (wt %)		AMC/DMAc/TEG (12 : 78 : 10)	PVDF/DMAc/PVP (14/80/6)
Pressure of TIPS dope (kgf/cm^2)	3	3	3
Pressure of NIPS dope (kgf/cm^2)		0.8	1
Bore fluid composition (wt %)	DMAc/TEG (50 : 50)	DMAc/TEG (50 : 50)	DMAc/EG (30/70)
Bore fluid flow rate (ml/min)	6	6	5
Air gap (mm)	0.8	0.8	5
Take-up speed (m/min)	20	20	30
External coagulant composition (wt %)	Water/DMAc (100/0, 80/20, 50/50)	Water	water
Dope temperature of TIPS (K)	393	393	403
Dope temperature of NIPS (K)	313	313	313
Bore fluid temperature (K)	353	353	323
External coagulant temperature (K)	313	313	293
Dimension of spinneret (mm)	i.d./o.d. (2.0/4.1)	i.d./o.d. (2.0/5.1)	i.d./o.d. (2.0/4.1)

Matsuyama *et al.*[21] achieved the first hydrophilic cellulose acetate hollow fiber membrane by liquid–liquid phase separation using TIPS, and showed that the membrane had isotropic pore structure without the formation of macrovoids. Fu *et al.*[23] studied the effect of membrane preparation method on the outer surface roughness of cellulose acetate butyrate hollow fiber membranes prepared via TIPS and NIPS.

Hollow fiber membranes fabricated by the TIPS process tend to have high tensile strength, but the pores are too large to retain polymeric molecules. In contrast, the hollow fiber membranes prepared by the NIPS process can have smaller pores than those produced by the TIPS process, but the tensile strength is much lower. The dual-layer hollow fiber membrane prepared by both NIPS and TIPS processes can have both small pores and high tensile strength. Furthermore, the co-extrusion method allows the dual-layer membrane to possess the advantages of each individual layer.[26] Liu *et al.*[27] prepared a dual-layer hollow fiber ultrafiltration membrane with PVDF dope solutions via the TIPS method, and then fabricated a second layer with PES dope solutions through the NIPS method in a two-step process. In another study, Liu *et al.*[28] prepared polyvinyl chloride (PVC) matrix reinforced hollow fiber membranes including a separation layer and a porous supported matrix via the two-step process. The porous inner layer works as a mechanical support for the selective outer skin layer.[29] Various studies have reported the use of polymeric dual-layer hollow fiber membranes for wastewater treatment, nanofiltration,[30] gas separation,[31–33] forward osmosis,[34] membrane distillation,[35,36] pervaporation,[37] and biomedical applications.[38] However, dual-layer hollow fiber membranes made with cellulosic polymers have rarely been reported in the literature. Sun *et al.*[29] reported the fabrication of a dual-layer nanofiltration hollow fiber membrane by the simultaneous co-extrusion (one-step) of polyamide-imide and cellulose acetate dopes through a triple-orifice spinneret in a dry-jet wet phase inversion process. However, the major issue facing dual-layer composite membranes is the adhesion of the two layers and integrity of the membrane.[39]

The objective of this study was to fabricate a dual-layer acetylated methyl cellulose (AMC) hollow fiber membrane with enhanced mechanical strength and fouling resistance. To the best of our knowledge, this is the first report of a dual-layer hollow fiber membrane based on cellulosic polymers with two different phase inversion pathways. A one-step co-extrusion method was applied for fabrication of dual-layer hollow fiber membranes to improve the ultrafiltration properties of the membrane. A novel dual-layer AMC hollow fiber membrane was fabricated by forming the inner layer via the TIPS method, followed by formation of the outer layer with the NIPS method. The mechanical properties, morphology, and performances of the prepared dual-layer membranes were systematically characterized. We consider this as an important step in engineering cellulosic polymer membranes into affordable devices.

EXPERIMENTAL

Materials

Acetylated methyl cellulose (AMC, Mw of 370 kDa) was supplied by Samsung Fine Chemical Corporation, Korea. *N,N*'-dimethylacetamide (DMAc), triethylene glycol (TEG), poly(vinyl pyrrolidone) (PVP, MW of 30 kDa), and γ-butyro lactone (GBL) were purchased from Sigma-Aldrich. Poly(vinylidene difluoride) (PVDF, Mw of 500 kDa) was purchased from Solvay, Japan. Deionized water from Millipore systems was used as the non-solvent in the coagulation bath.

Membrane Preparation

Prior to the preparation of TIPS/NIP combined dual-layer fiber, TIPS layer was fabricated to investigate the effect of preparation conditions on membrane structure. For the TIPS process, AMC was added in TEG solvent and the mixture was stirred at 393 K for 4 h under a nitrogen condition. The doping solution and

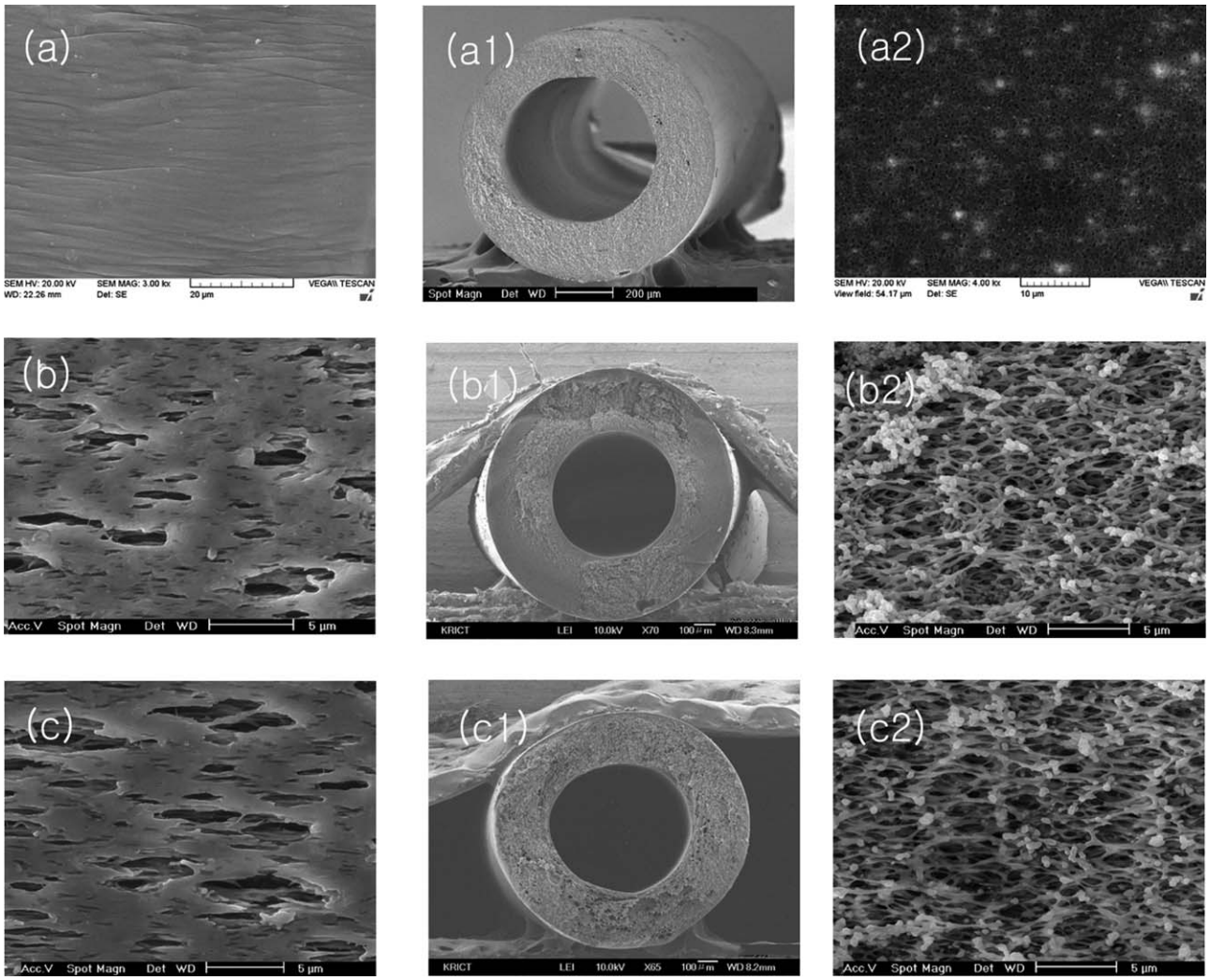

Figure 1. SEM photographs of the AMC membranes fabricated by the TIPS process: (a) outer surface, (a1) cross-section, and (a2) inner surface of the membranes coagulated in water; (b) outer surface, (b1) cross-section, and (b2) inner surface of the membranes coagulated in 20 wt % DMAc solution; (c) outer surface, (c1) cross-section, and (c2) inner surface of the membranes coagulated in 50 wt % DMAc Solution.

inner coagulant (bore solution) were extruded through the outer and the inner channels of a spinneret under the nitrogen pressure of 3 kgf/cm^2. The spinneret had outer and inner diameters of 4.1 and 2.0 mm, respectively. The compositions of the dope used for the TIPS process and the bore solution were AMC/TEG (25/75 wt %) and DMAc/TEG (50/50 wt %), respectively. The coagulation bath contained various amounts of DMAc solvent in water, and the temperature of the bath was maintained at 293 K. The water/DMAc weight ratios in the bath were set at 100/0, 80/20, and 50/50, and the solidified fiber in coagulation bath was taken up at the speed of 20 m/min.

After finding the proper fabrication condition of TIPS process, TIPS/NIPS dual-layered hollow fiber membranes were prepared. The composition of the dope for the NIPS process was AMC/DMAc/TEG (12/78/10 wt %) except when checking the effect of TEG content on its performance. The composition of TIPS solution AMC/TEG (25/75 wt %). The TIPS solution was fed to a spinneret by extruding under the nitrogen pressure of 3 kgf/cm^2 and NIPS solution was fed to a spinneret by extruding

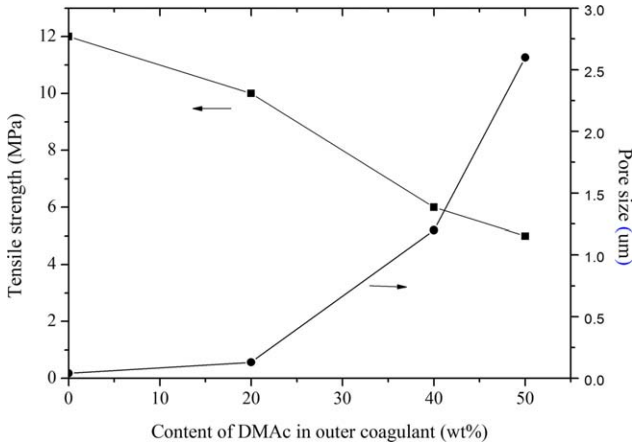

Figure 2. Tensile strength and pore size of the AMC membranes fabricated with different solvent content in external coagulant. [Color figure can be viewed in the online issue, which is available at wileyonlinelibrary.com.]

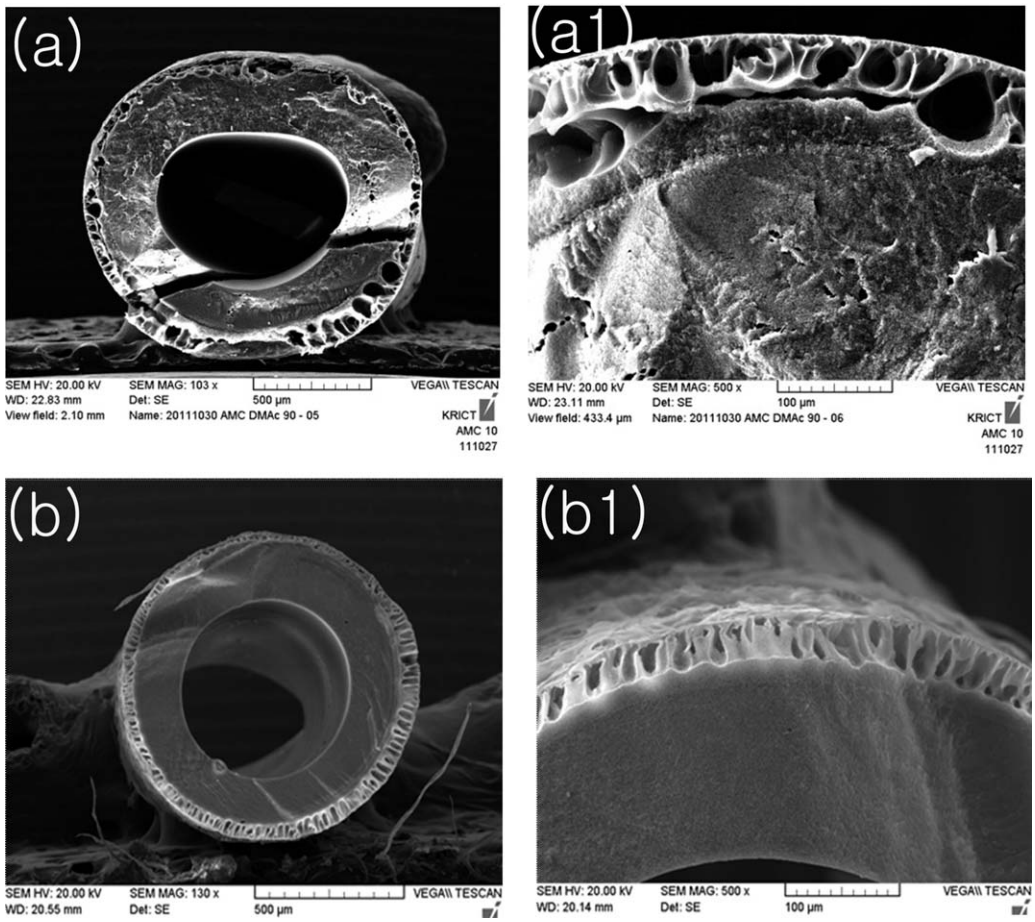

Figure 3. Cross-sectional images of the dual-layer AMC hollow fiber membrane: (a) no TEG in NIPS solution, (a1) enlarged cross-section of (a), (b) TEG in NIPS solution, and (b1) enlarged cross-section of (b).

under the nitrogen pressure of 0.8 kgf/cm^2. As an inner coagulant, DMAC/TEG mixture of 50/50 was used for spinning condition with a fixed air gap of 0.8 cm. The coagulation bath composed of water. The diluent remaining in the hollow fiber product was extracted by immersion in water for 24 h.

In order to compare the prepared AMC membrane with PVDF hollow fiber membranes, a dual-layer PVDF hollow fiber membrane was also fabricated with the same procedure as the dual-layer AMC membranes. Table I shows the spinning conditions for the AMC and PVDF dual-layer hollow fiber membranes.

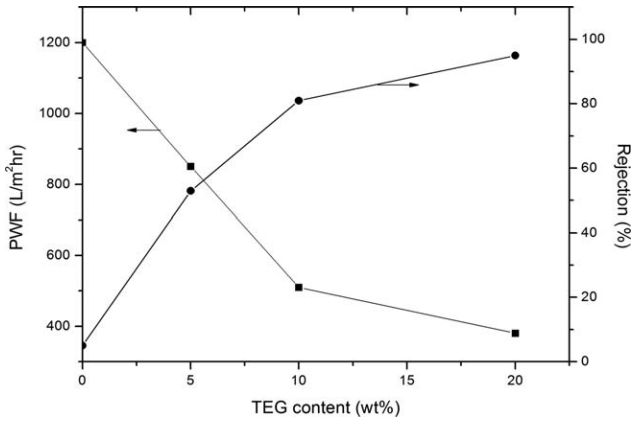

Figure 4. Effect of TEG addition to the NIPS solution on the performance of dual-layer AMC hollow fiber membranes.

Membrane Characterization

The structure and morphology of the dual-layer hollow fiber membrane were characterized by field emission scanning electron microscope (FE-SEM) using a Tescan Mira 3 LMU FEG operated at an acceleration voltage of 10 kV. The FE-SEM samples were prepared by vacuum sputtering Pt onto the dried samples at room temperature. Atomic Force Microscopy (AFM) was applied for determination of the surface roughness of the hollow fiber membranes using a Multimode V (Veeco, USA). Tensile strength tests were conducted at a load speed of 50 mm/min with 50 mm lengths of samples until specimen breakage occurred. Pure water flux and rejection of polyethylene oxide (PEO, MW of 100 kDa, Sigma-Aldrich) of the hollow fiber membranes were also measured. Pure water or PEO solution was introduced from the outside to the inside of the dual-layer hollow fiber membranes at the conditions of 1 kgf/cm^2 and 1 L/min. Rejection of PEO was measured using HPLC.

In order to measure the contact angle, the membranes were fixed on a cover glass and then immersed in isoparaffin (SKC, Korea) solution. After 1 h, a droplet of ethylene glycol (Sigma-

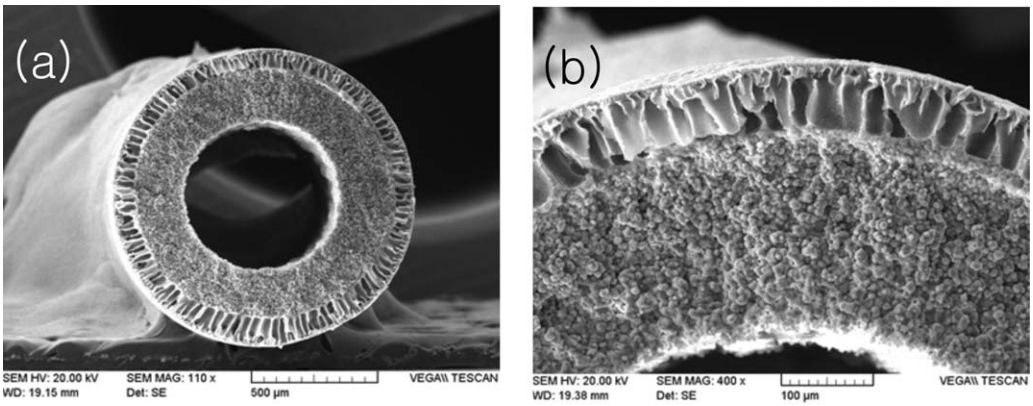

Figure 5. Cross-sectional images of the dual-layer PVDF hollow fiber membrane: (a) overall cross-section, and (b) enlarged cross-section of (a).

Aldrich) was placed on the membrane sample. Two membrane replicates were used, with measurement and averaging of five drops per replicate. Membrane fouling experiments were conducted with 20 ppm of bovine serum albumin (BSA, Sigma-Aldrich). The water flux decrease due to BSA fouling was measured for 2 h at 1 kgf/cm^2 and 1 L/min.

RESULTS AND DISCUSSION

Optimization of AMC TIPS Layer

Prior to the fabrication of AMC hollow fibers with TIPS and NIPS dual-layers, optimization of the TIPS layer was conducted.

It is well known that increase of the polymer concentration at the interface of the polymer solution resulting from lower exchange of the solvent with the non-solvent during the precipitation process leads to the formation of a non-porous, dense active layer. To inhibit the formation of a dense skin layer, which is unfavorable for porous membranes, the polymer solution was spun into coagulation baths with various compositions of water/DMAc, and the effects of coagulation bath composition on the membrane structures were investigated. As shown in Figure 1, no large spherulites could be found in the cross-section or inner surface of the hollow fiber membrane, indicating that the AMC polymer solution resulted in liquid–liquid phase separation instead of solid–liquid phase separation from crystallization. The liquid–liquid phase separation divided the homogeneous solution into two phases, an AMC-rich phase and a TEG-rich phase, before solidification. This allowed the membrane structure to be bicontinuous, resulting in hollow fibers without the production of nucleation and growth of the AMC polymer.

Table II. Comparison of the Properties of the Two Hollow Fiber Membranes

Hollow fibers	PWF (LMH)	Rejection of PEO 100 kDa (%)	Tensile strength (MPa)	Roughness (Ra, nm)
AMC	510	81	8.5	2.12
PVDF	650	85	6.3	4.39

In the case of the coagulation bath composed of only water, the AMC membrane exhibited a symmetric cellular structure, composed of a dense active layer. Upon immersion of the polymeric solution in the 100% water coagulation bath, fast exchange between the solvent and non-solvent occurred across the interface. The role of the TIPS layer is to give the hollow fiber high tensile strength by increasing the polymer concentration. Exposure of the TIPS solution to a strong non-solvent causes the polymers to have strong entanglement with each other. As a result, a dense surface and sponge-like pores with small pore size were formed. After immersed in a bath containing 20 wt % DMAc, larger pores on the membrane surface appeared, as represented in the Figure 1. With further increase of the DMAc concentration to 50%, more pores were formed on the membrane surface, and the pore size also became larger. It was also found that the pore size at the outer surface was smaller than that at the inner surface. The addition of solvent into the immersion precipitation bath delayed solidification of the polymer, which caused the polymer concentration on the membrane surface to decrease. The resulting hollow fiber membrane showed a porous structure at the outer surface, as well as at the inner surface of the membrane. However, a clear trend appeared

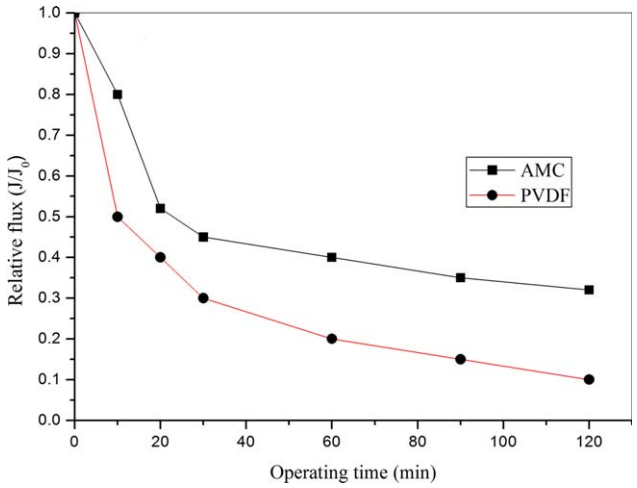

Figure 6. Relative fluxes of AMC and PVDF hollow fiber membranes. [Color figure can be viewed in the online issue, which is available at wileyonlinelibrary.com.]

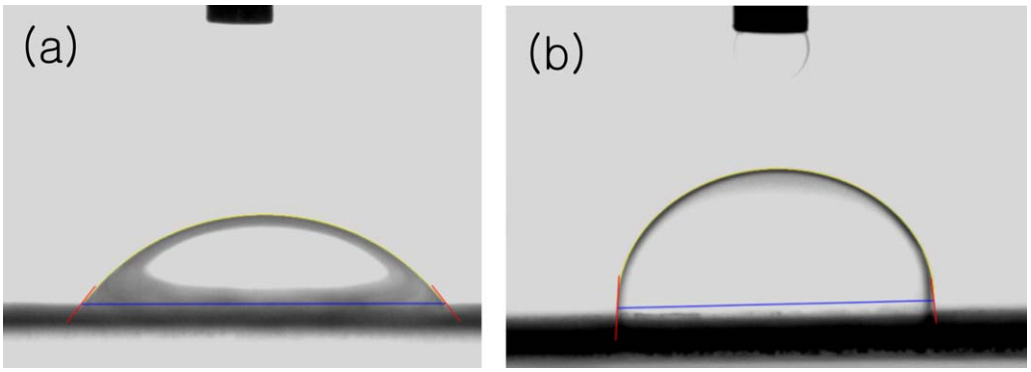

Figure 7. Contact angle of (a) AMC and (b) PVDF hollow fiber membranes. [Color figure can be viewed in the online issue, which is available at wileyonlinelibrary.com.]

that increase of the DMAc concentration in the coagulation bath led to decrease of the tensile strength and increased pore size with loose structure, as illustrated in Figure 2.

Fabrication of TIPS and NIPS Dual-Layer Membrane

Dual-layer AMC hollow fiber membranes were prepared via a combination of the TIPS and NIPS processes in a single process. Figure 3(a) shows the cross-sectional images of the dual-layer AMC hollow fiber membrane, which was fabricated in absence of TEG in NIPS solution. The interface between the TIPS and NIPS layers was separated them from each other. Because of the different phase separation rates between the TIPS and NIPS solutions, the adhesion stability of the two was poor. In order to enhance the adhesion stability, the diluent, TEG, used in the TIPS solution was added to the NIPS solution. As can be seen in Figure 3(b), the interface between the TIPS and NIPS layers could be completely interconnected through this method. This is likely due to easy mixture of TIPS solution and NIPS solution at the interface. The inner side of TIPS solution can solidify first due to contact with an inner coagulant (bore solution), after which phase separation of the NIPS solution can occur due to contact with an outer coagulant. The use of the diluent in the NIPS solution resulted in TEG transfer from temperature elevated TIPS solution to the NIPS solution during phase inversion, leading to the entanglement of polymers between TIPS and NIPS solutions.

Figure 4 shows the permeation performance of the dual-layer hollow fiber membranes at different TEG contents in the NIPS solution. The results indicate that increasing TEG content in the NIPS solution caused decreased flux and pore size of the dual-layer hollow fiber membranes. The increased adhesion stability might reduce the production of large vacant voids between the NIPS and TIPS layers. Instead of the large voids, an interconnected layer of the two solutions can be formed. Interconnection of the two layers may reduce the flow channels and decrease the water flux. Moreover, the defects in the interface completely disappeared, which could support enhanced rejection of polymeric molecules.

Fouling of the AMC Dual-Layer Hollow Fiber Membrane

Fouling of the AMC dual-layer hollow fiber membrane was compared with that of the PVDF dual-layer hollow fiber membrane.

PVDF has enjoyed wide use as a membrane material for water treatment. However, PVDF membranes are very sensitive to membrane fouling due to their hydrophobic properties. Accordingly, many researchers have modified the materials to control fouling. The PVDF dual-layer hollow fiber membrane was fabricated using the same method as the AMC dual-layer hollow

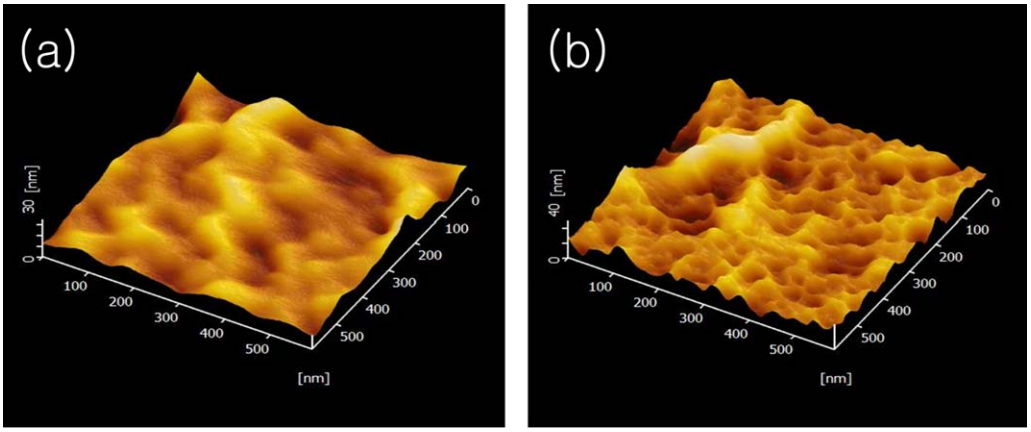

Figure 8. AFM pictures of (a) AMC and (b) PVDF hollow fiber membranes. [Color figure can be viewed in the online issue, which is available at wileyonlinelibrary.com.]

fiber membrane, after which the two types of membranes were compared. The composition of the PVDF casting solution was determined for fabrication of membranes with similar permeation properties as the AMC hollow fiber membrane. Figure 5 shows the SEM pictures of the PVDF dual-layer hollow fiber membrane. The TIPS cross-sectional structure of the PVDF hollow fiber membrane was looser than that of the AMC hollow fiber membrane, while the NIPS layer showed the finger-like structure. The NIPS layer was completely connected with the TIPS layer in the PVDF membrane. Comparison of the properties of the two hollow fiber membranes is shown in Table II. The pure water flux and rejection of PEO 100 kDa was similar. However, the tensile strength of the AMC hollow fiber membrane was higher than that of the PVDF hollow fiber membrane.

The fouling of the AMC and the PVDF hollow fiber membranes was investigated and shown in Figure 6. The PVDF hollow fiber membrane was heavily fouled due to its protein adsorption, displaying a decrease in the flux to one-tenth after 2 h. In contrast, the AMC hollow fiber membrane became less fouled than the PVDF hollow fiber membrane, with a decrease to 40% flux after 2 h. In order to determine the reasons for this fouling difference, contact angles and AFM pictures were taken, as shown in Figure 7. From the contact angle, it could be confirmed that the AMC hollow fiber membrane was more hydrophilic than the PVDF hollow fiber membrane. In general, it is widely known that cellulosic polymers are hydrophilic and have smooth surfaces, causing them to be fouled less. AMC is also a cellulosic polymer. Methyl cellulose (MC), which is soluble in water, is partially substituted with acetyl groups. AMC is more hydrophobic than MC. However, AMC is more hydrophilic than PVDF, which is widely used as a membrane material. In comparison, PVDF contains a fluoro group, which is water repellent and highly hydrophobic. From the AFM pictures of Figure 8, it was determined that the roughness of the AMC hollow fiber membrane was lower than that of the PVDF hollow fiber membrane, which means that the AMC membrane was smoother. The roughness data are summarized in Table II. The phase inversion rate of the AMC membrane may be faster than that of the PVDF membrane. As AMC is a hydrophilic polymer, coagulant water can approach the AMC solution more easily during the phase inversion process, allowing formation of a smoother surface. In contrast, PVDF is a hydrophobic polymer, which means that the PVDF hollow fiber membrane solidified slowly due to its water repellent property. As a result, the surface of the PVDF membrane could be rougher.

CONCLUSION

Acetylated methyl cellulose (AMC) was used as a new membrane material. AMC hollow fiber membranes with a coating layer placed on a support layer were prepared by the thermally induced phase separation (TIPS) and non-solvent induced phase separation (NIPS) methods through a co-exclusion process. Moreover, a PVDF dual-layer hollow fiber membrane with good adhesion stability was fabricated for comparison of the fouling resistance. In the case of AMC hollow fiber membranes, liquid–liquid phase separation was observed. As the concentration of solvent in the coagulation bath containing a non-solvent increased, the membrane morphology became more porous. Structures that are more porous causes the membrane to have weak mechanical strength. However, the composite AMC hollow fiber membrane with dual-layers had good mechanical strength, as well as finger-like porous structure. The addition of TEG to the NIPS solution could enhance the adhesion stability between the TIPS and NIPS layers. It was confirmed that the coating layer could successfully adhere to the support layer via the TIPS process, as revealed by SEM. The AMC hollow fiber membrane displayed better fouling resistance than the PVDF hollow fiber membrane. It seems that the better fouling resistance resulted from the higher hydrophilicity and smoother surface of the AMC hollow fiber membrane.

ACKNOWLEDGMENTS

This research was supported by the World Premier Materials Program through the Ministry of Trade Industry & Energy and supported by the R&D Center for Valuable Recycling (Global-Top R&D Program) of the Ministry of Environment [Project No.2014001160002]. The authors are grateful for support from these organizations.

REFERENCES

1. Kuo, Y. N.; Hong, J. *J. Colloid Interface Sci.* **2005**, *285*, 232.
2. Jayalakshmi, A.; Rajesh, S.; Kim, I. C.; Senthilkumar, S.; Mohan, D.; Kwon, Y. N. *J. Membr. Sci.* **2014**, *465*, 117.
3. Kastelan Kunst, L.; Dananic, V.; Kunst, B.; Kosutic, K. *J. Membr. Sci.* **1996**, *109*, 223.
4. Saljoughi, E.; Sadrzadeh, M.; Mohammadi, T. *J. Membr. Sci.* **2009**, *326*, 627.
5. Sivakumar, M.; Mohan, D. R.; Rangarajan, R. *J. Membr. Sci.* **2006**, *268*, 208.
6. Mu, C.; Su, Y.; Sun, M.; Chen, W.; Jiang, Z. *J. Membr. Sci.* **2010**, *350*, 293.
7. Qin, J. J.; Li, Y.; Lee, L. S.; Lee, H. *J. Membr. Sci.* **2003**, *218*, 173.
8. Razzaghi, M. H.; Safekordi, A.; Tavakolmoghadam, M.; Rekabdar, F.; Hemmati, M. *J. Membr. Sci.* **2014**, *470*, 547.
9. Shibutani, T.; Kitaura, T.; Ohmukai, Y.; Maruyama, T.; Nakatsuka, S.; Watabe, T.; Matsuyama, H. *J. Membr. Sci.* **2011**, *376*, 102.
10. Feng, C. S.; Wang, R.; Shi, B. L.; Li, G. M.; Wu, Y. L. *J. Membr. Sci.* **2006**, *277*, 55.
11. Han, J.; Yang, D.; Zhang, S.; Jian, X. *J. Membr. Sci.* **2009**, *345*, 257.
12. vandeWitte, P.; Dijkstra, P. J.; vandenBerg, J. W. A.; Feijen, J. *J. Membr. Sci.* **1996**, *117*, 1.
13. Caplan, M. R.; Chiang, C. Y.; Lloyd, D. R.; Yen, L. Y. *J. Membr. Sci.* **1997**, *130*, 219.
14. Liu, F.; Hashim, N. A.; Liu, Y.; Abed, M. R. M.; Li, K. *J. Membr. Sci.* **2011**, *375*, 1.
15. Luo, B. Z.; Zhang, J.; Wang, X. L.; Zhou, Y.; Wen, J. Z. *Desalination* **2006**, *192*, 142.

16. Yang, Z. S.; Li, P. L.; Xie, L. X.; Wang, Z.; Wang, S. C. *Desalination* **2006**, *192*, 168.
17. Ramaswamy, S.; Greenberg, A. R.; Krantz, W. B. *J. Membr. Sci.* **2002**, *210*, 175.
18. Roh, I. J.; Ramaswamy, S.; Krantz, W. B.; Greenberg, A. R. *J. Membr. Sci.* **2010**, *362*, 211.
19. Cha, B. J.; Yang, J. M. *J. Membr. Sci.* **2007**, *291*, 191.
20. Rajabzadeh, S.; Maruyama, T.; Sotani, T.; Matsuyama, H. *Separ. Purif. Tech.* **2008**, *63*, 415.
21. Matsuyama, H.; Ohga, K.; Maki, T.; Tearamoto, M.; Nakatsuka, S. *J. Appl. Polymer Sci.* **2003**, *89*, 3951.
22. Fu, X.; Maruyama, T.; Sotani, T.; Matsuyama, H. *J. Membr. Sci.* **2008**, *320*, 483.
23. Fu, X. Y.; Sotani, T.; Matsuyama, H. *Desalination* **2008**, *233*, 10.
24. Matsuyama, H.; Takida, Y.; Maki, T.; Teramoto, M. *Polymer* **2002**, *43*, 5243.
25. Wu, Q.-Y.; Wan, L.-S.; Xu, Z.-K. *J. Membr. Sci.* **2012**, *409*, 355.
26. Li, D. F.; Chung, T. S.; Rong, W. *J. Membr. Sci.* **2004**, *243*, 155.
27. Liu, T.-Y.; Zhang, R.-X.; Li, Q.; Van der Bruggen, B.; Wang, X.-L. *J. Membr. Sci.* **2014**, *472*, 119.
28. Liu, H.; Xiao, C.; Huang, Q.; Hu, X.; Shu, W. *J. Membr. Sci.* **2014**, *472*, 210.
29. Sun, S. P.; Wang, K. Y.; Peng, N.; Hatton, T. A.; Chung, T.-S. *J. Membr. Sci.* **2010**, *363*, 232.
30. He, T.; Mulder, M. H. V.; Strathmann, H.; Wessling, M. *J. Membr. Sci.* **2002**, *207*, 143.
31. Ding, X.; Cao, Y.; Zhao, H.; Wang, L. *J. Membr. Sci.* **2013**, *444*, 482.
32. Li, F. Y.; Li, Y.; Chung, T.-S.; Chen, H.; Jean, Y. C.; Kawi, S. *J. Membr. Sci.* **2011**, *378*, 541.
33. Peng, N.; Chung, T.-S.; Chng, M. L.; Aw, W. *J. Membr. Sci.* **2010**, *360*, 48.
34. Yang, Q.; Wang, K. Y.; Chung, T.-S. *Environ. Sci. Technol.* **2009** *43*, 2800.
35. Bonyadi, S.; Chung, T.-S. *J. Membr. Sci.* **2009**, *331*, 66.
36. Setiawan, L.; Shi, L.; Krantz, W. B.; Wang, R. *J. Membr. Sci.* **2012**, *423*, 73.
37. Ong, Y. K.; Chung, T.-S. *J. Membr. Sci.* **2012**, *421*, 271.
38. Hilke, R.; Pradeep, N.; Behzad, A. R.; Nunes, S. P.; Peinemann, K.-V. *J. Membr. Sci.* **2014**, *472*, 39.
39. Setiawan, L.; Wang, R.; Shi, L.; Li, K.; Fane, A. G. *J. Membr. Sci.* **2012**, *421*, 238.